Painted supported lipid membranes

E.-L. Florin and H. E. Gaub*
Physikdepartment Technische Universität München, 8046 Garching, Germany

ABSTRACT We report herein measurements on a novel type of supported lipid films, which we call painted supported membranes (PSM). These membranes are formed in a self-assembly process on alkylated gold films from an organic solution. The formation process was investigated with surface plasmon resonance microscopy. The optical and electrical properties of the films were determined for various types of lipids and as a function of temperature by means of cyclic voltammetry and potential relaxation after charge injection. We could show that these films exhibit an extraordinarily high specific resistivity which, depending on the lipid, may be as high as 10^9 ohm/cm^2. We could also show that due to this low conductivity, an electrical polarization across the PSM relaxes with characteristic time constants of up to 20 min. The electrical properties together with their high mechanical stability and accessibility to surface sensitive techniques make these films well suitable model membranes for optical and electrical investigations. Examples for such applications are given in the subsequent article by Seifert et al.

INTRODUCTION

Freestanding bimolecular lipid films are widely used model systems for cell membranes. A rich body of literature exists, where such membranes have been used to measure the electrical properties mainly of ion channels and carriers or of ATP-ases which were either incorporated into the films or which were imbedded in associated membrane fragments or partially fused vesicles (1–3). One variant of these free standing films, the BLM (4) is widely used because of its ease to form and its comparably large size of up to several square millimeters. Their major drawback, however, is their lack in mechanical stability. The surface tension between film and water which is on the order of 30–40 mN/m tries to minimize the area of the film and thus tends to rip open holes which might be caused by fluctuations or mechanical disturbances. The rim tension of such a hole tends to minimize the amount of exposed hydrocarbon area to water and tries conversely to close the hole again. The first term depends quadratically on the radius r of a hole, whereas the second term depends linearly on the diameter of the hole. In a zero order approximation the energy will therefore be of the form:

$$E_{\mathrm{BLM}} = 2R - R^2, \qquad (1)$$

where $R = r/r_{\max}$ is the radius normalized on the maximum stable pore radius, which is determined by the rim tension and the surface tension as follows: $r_{\max} = \Gamma_{\mathrm{rim}}/E_{\mathrm{lipid/water}}$. With literature values (5) for $\Gamma_{\mathrm{rim}} = 4.2 \cdot 10^{-20}$ J/nm and $E_{\mathrm{lipid/water}} = 40$ mJ/m^2, the maximum radius is on the order of 1 nm. The energy is normalized on the maximum energy at $r_{\max}$: $E_{\mathrm{BLM}} = E(R)/\pi \cdot \Gamma^2_{\mathrm{rim}}/E_{\mathrm{lipid/water}}$. This dependence of the energy on the radius of the pore is depicted in Fig. 1. It shows that the membrane is stable only up to a certain pore size and will rupture above this maximum value.

In order to overcome this instability we have designed a new type of membrane: a painted supported membrane. Here the hydrocarbon chains of the membrane are chemically bound to a solid support on one side of the film (see Fig. 2). Large lateral density fluctuations of the covering lipid film will, in this case, expose hydrophobic surfaces of the bound chains to water. The resulting energy will be of the form:

$$E_{\mathrm{PSM}} = 2R + vR^2 - R^2, \qquad (2)$$

and will therefore monotonically increase with the pore size, resulting in an improved stability of the membrane (see Fig 1). The second term in Eq. 2 is the additional energy due to the exposure of the hydrophobic surface. v is the ratio of the surface free energies of the water/hydrocarbon interface and the lipid/water interface, which is on the order of 2.

An additional advantage of this concept, to paint the membrane onto a solid support, arises from the possibility to employ surface sensitive techniques, which have been developed in recent years in a broad variety, for the investigations of and with such films. These aspects will be exploited in the following experiments.

MATERIALS AND METHODS

Chemicals

Ethanol absolute p.a. (Riedel-de Haën AG, Seelze, Germany), Hexadecylmercaptane (HDM) technical grad 92% (Aldrich-Chemie GmbH, Steinheim, Germany), Dimethyl-dichlorosilane (>99.5%) (Fluka AG, Neu-Ulm, Germany), decane (oelifine free >99%) (Fluka AG) sodium chloride p.a. (E. Merck, Darmstadt, Germany). Potassium chloride p.a. (Sigma GmbH, Deisenhofen, Germany), potassium-hexacyanoferrate (II) p.a. (Fluka AG), hellmanex (Hellma GmbH&Co, Müllheim, FRG), L-α-Dilauroyl phosphatidylcholine (DLPC) (synthetic: ~99%) (Sigma Chemie GmbH), L-α-Dimyristoyl phosphatidylcholine (DMPC) (synthetic: ~99%) (Sigma Chemie GmbH), L-α-Dipalmatoyl phosphatidylcholine (DPPC) (synthetic: ~99%) (Sigma Chemie GmbH), L-α-Dioleoyl phosphatidylcholine (DOPC) (synthetic: ~99%) (Sigma Chemie GmbH) and 1-palmitoyl-2(6-((7-nitro-2-1,3-benzoxadiazol-4-yl)amino)caproyl)-posphatidylcholin (Avanti Polar Lipids, Birmingham, AL) were used without further purification.

* To whom correspondence should be addressed.

0006-3495/93/02/375/09 $2.00

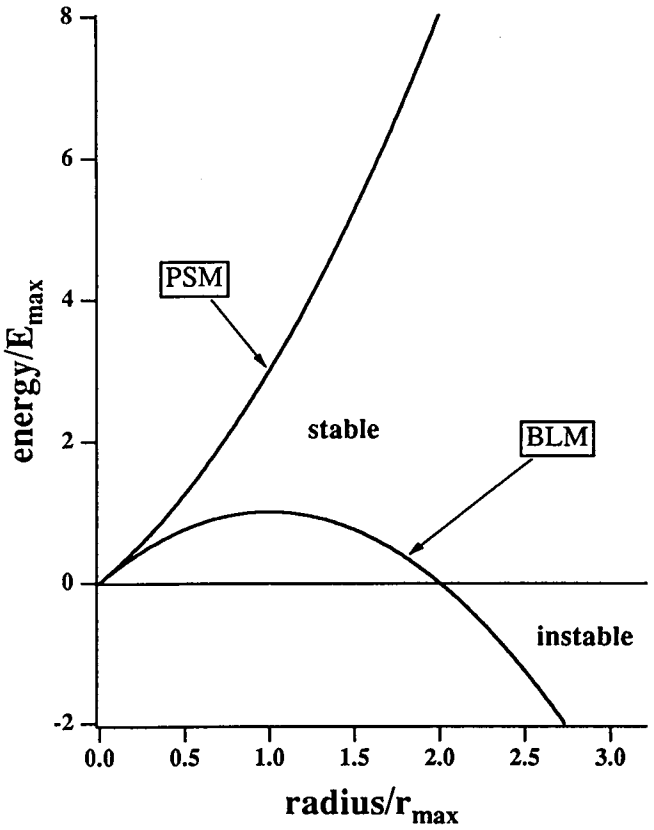

FIGURE 1 First order stability analysis of a hole with radius r in a free standing lipid membrane and in a painted supported membrane.

Preparation of the samples

All substrates, prisms (Spindler and Hoyer, Göttingen, Germany, SF10, n = 1.7343, 30 × 30 mm) and quartz slides (Heräus Quarzschmelze, Hanau, Germany), were cleaned as follows: (*a*) 15 min ultrasonicated in 2% Hellmanex solution; (*b*) washed with pure water (Milli Pore-quality); (*c*) 15 min ultrasonicated in millipore water; (*d*) 15 min ultrasonicated in 2% Hellmanex solution; (*e*) rinsed with millipore water; (*f*) 15 min ultrasonicated in millipore water; (*g*) rinsed with millipore water; (*h*) dried at 70°C in a heat chamber overnight or alternatively in a vacuum chamber at room temperature for at least 3 h. As a last step, the substrates were rendered hydrophobic by brief exposure to dimethyl-dichlorosilane vapor. Clean samples were stored in dust free containers for less than one week. High purity gold (99,999%) was deposited by thermal evaporation at $3 \cdot 10^{-6}$ mbar pressure. Occasionally the samples were stored several days before alkylation. For alkylation we (*a*) filled up the containers with ethanol; (*b*) added hexadecylmercaptane (1% vol solution) a few minutes later; (*c*) removed the samples and rinsed them with ethanol prior to drying in air. Advancing contact angle measurements with millipore water were used to confirm the alkylation (typically 111°) (see also reference 6). Sample chambers (PMMA rings with an inner diameter of 5 mm) were glued on the surface with a two component epoxy resin (see Fig. 3). The residual uncovered area was between 1 mm² and 15 mm². Working electrodes for electrochemical measurements were thermally plated by evaporating a 1,000 Å gold film onto microscope slides with an area of 0.5 cm². The electrodes were coated with HDM with the following procedure: (*a*) heating up the electrode in ethanol absolute well below the boiling point; (*b*) adding HDM; (*c*) cooling down to room temperature; (*d*) removing the electrode out of the beaker after minimal 30 min; (*e*) rinsing the slide with ethanol and (*f*) blowing dry with nitrogen gas.

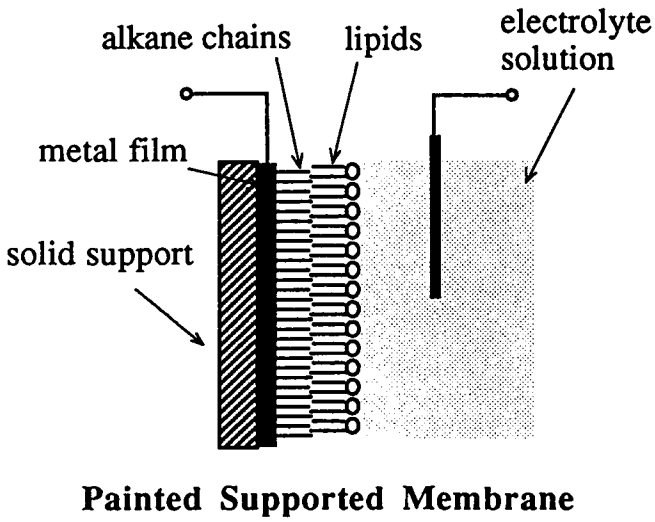

FIGURE 2 Schematics of a painted supported membrane (PSM).

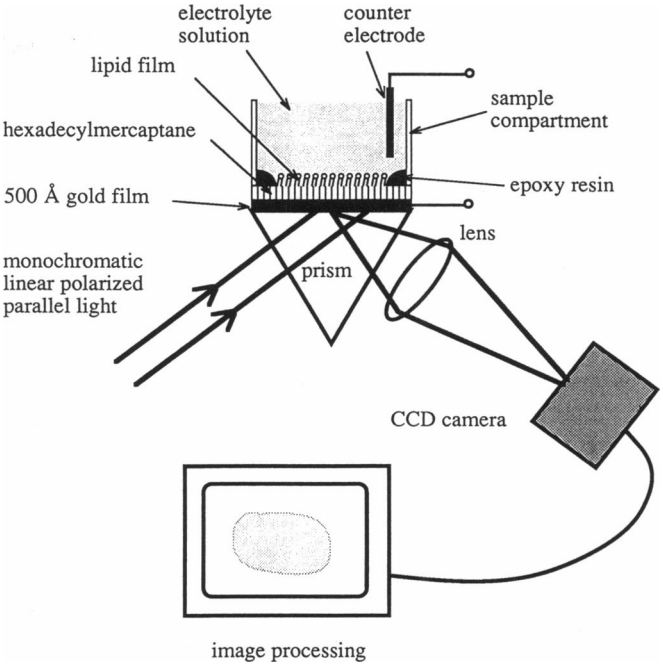

FIGURE 3 Schematics of the surface plasmon microscopy set-up used in this study.

Capacitance measurements

The capacitance of the membranes was determined by measuring the relaxation time τ of the RC-circuit. Two different configurations were used: (*a*) a square wave with an amplitude of ±100 mV and a frequency between 50 and 100 Hz was applied and the voltage drop across an external resistor of R_e = 10 kΩ, was measured with a storage oscilloscope (Hameg HM 203-7; Hameg, Frankfurt). (*b*) an electrometer (Keithley 610 C; Keithley Instruments GmbH, München) connected to an x-t-plotter after a potential jump of less than 100 mV had been applied. In both cases we calculated the membrane capacitance with a

simple model of a RC-circuit neglecting the resistance of the counter electrode, the resistance of the electrolyte and the capacitance of the counter electrode (only in the asymmetric design). In the case of the symmetric design the two membranes were in series and were treated accordingly. The capacitance of the counter electrode was in a series to the membrane capacitance but under our experimental conditions it was about a hundred times larger than the membrane capacitance and was therefore neglected. The electrolyte resistance which was also in series to the membrane resistance is small compared to the external resistance R_e and was therefore neglected too. For the calculation of the specific capacitance the membrane area was measured by surface plasmon microscopy.

Conductivity measurements

The membrane conductivity was determined by three different methods: (*a*) by directly measuring the current versus voltage characteristics using an electrometer and a battery with a resistor bridge as power supply. For small voltages the current turned out to be approximately proportional to the applied voltage and the slope represents therefore the conductance. (*b*) by measuring the relaxation of the membrane potential after charging the membrane capacitance to a given voltage. The slope at $t = 0$ s yields the relaxation time. With the known capacitance, the membrane resistance is then given by $R_m = \tau / C_m$. (*c*) by measuring the difference ΔU between applied external voltage and maximal membrane potential after charging the membrane capacitance via an external resistant R_e to a defined voltage. The membrane resistance is given by $R_m = R_e(U_e/\Delta U - 1)$. Best accuracy is obtained with $R_m \approx R_e$. This method although extremely time consuming was favored in order to reduce noise and to follow changes in membrane conductance. This method was also used for temperature dependent conductivity measurements.

Temperature dependent measurements

For temperature dependent measurements we mounted the samples on a copper block, which was temperature controlled via a thermostat (Julabo VC; Julabo, Seelbach, Germany). To avoid electrical contact, a thin PTFE foil of 0.5 mm thickness, mounted with heat conductive paste, separated the sample from the copper block. Temperature measurements were taken by a digital thermometer (Keithley 870 digital thermometer; Keithley Instruments GmbH, München). The error of temperature measurements in our experiments are estimated to be ±2° Celsius.

Cyclic voltammetry

Cyclic voltammograms were recorded with a home built potentiostat. A platinum wire (diameter 0.5 mm) was used as the counter electrode and a saturated calomel electrode (SCE) (B2910; Schott, Hofheim a. Ts, Germany) as reference electrode. The gold film with the PSM served as working electrode. Because of the small currents, an electrometer (Keithley 610 C, see above) was used as pre-amplifier. To shield stray fields, the experiments were performed in a Faraday cage. The potentiostat was controlled by a computer (Macintosh SE with Interface LAB-SE (National Instruments, Austin, TX)) which was also used for data acquisition from the electrometer. Corresponding routines were written with the program LAB VIEW SE, also from National Instruments. Because of the discrete output of the computer, the minimal step width in the output voltage was 8 mV. The current measurement was taken before each step and after relaxation of the capacitive current. Under our experimental conditions, this method is limited to scan rates of maximal 100 mV/s. For experiments with only HDM the specific current was calculated with the geometric area of the working electrode. In the case of PSM's made from DOPC, the capacitance was first measured as described before. The monolayer area was then calculated from the ratio of the measured specific capacitance to the expected specific capacitance of a monolayer without residual solvent. All electrolyte solutions were degassed in vacuum.

Surface plasmon spectroscopy and microscopy

The principle of the experimental set-up of the surface plasmon microscope (SPM) used in our studies is depicted in Fig. 3 (for details see reference 7). The painted supported membrane on a thin gold film is illuminated from the back side via a high index prism with monochromatic parallel light of a given polarization. The reflected light is projected onto a CCD camera. The incidence angle is tuned such that the resonance condition is fulfilled for areas which are covered by a monomolecular lipid film only. From these areas the reflection is thus drastically reduced, which makes them appear dark in the images shown in Fig. 4. For quantitative thickness measurements, the incidence angle was varied and the angle of minimum reflection was determined with a parabolic fit. The thicknesses were determined via a Fresnel simulation based on the following parameters: prism ($\epsilon = 2.969$), gold film ($\epsilon = -12.02 + i1.05$), HDM ($\epsilon = 2.1$), lipid ($\epsilon = 2.25$), water ($\epsilon = 1.79$). The simulated shift of the minimum turned out to be as large as 2.2°/100 Å lipid. Surface plasmon spectroscopy was performed with a similar instrument but with a focused excitation (for details see reference 8).

RESULTS AND DISCUSSION

Formation of PSMs

The formation of freestanding painted membranes is usually observed directly by light microscopy. The decrease of their reflectance upon thinning has given them their name. On conducting supports like metals, however, this effect is less well pronounced and other techniques must be applied in order to visualize and quantify the formation of a monomolecular lipid film.

The resonance of plasmonic surface polaritons or so called surface plasmons, is well established in the literature as a very sensitive indicator for thin dielectric layers on certain metals (9). Already a monomolecular lipid film results in a drastic change of the dispersion relation and thus of the resonance conditions of the surface plasmon. As has been shown by several authors, this resonance and its shift may be detected by measuring the reflectance of the metal film with monochromatic light as a function of the incidence angle (7, 10). The differences in the angular reflectance can also be used as contrast mechanism in microscopy (7)). For microscopy the sample is illuminated at a given angle and the local reflectivity is then converted into a thickness using model calculations based on the Fresnel equations. Fig. 3 shows the experimental set-up used in this study.

The formation of a PSM as seen with the surface plasmon microscope is depicted in Fig. 4. As support for the PSM a 500 Å thick, alkylated gold film on a high index glass prism was used with a small diaphragm and a sample compartment glued on top of the prism. The gold film was covered with a drop of the lipid solution and the sample chamber was then filled with the electrolyte solution. A voltage with a rectangular modulation of ±100

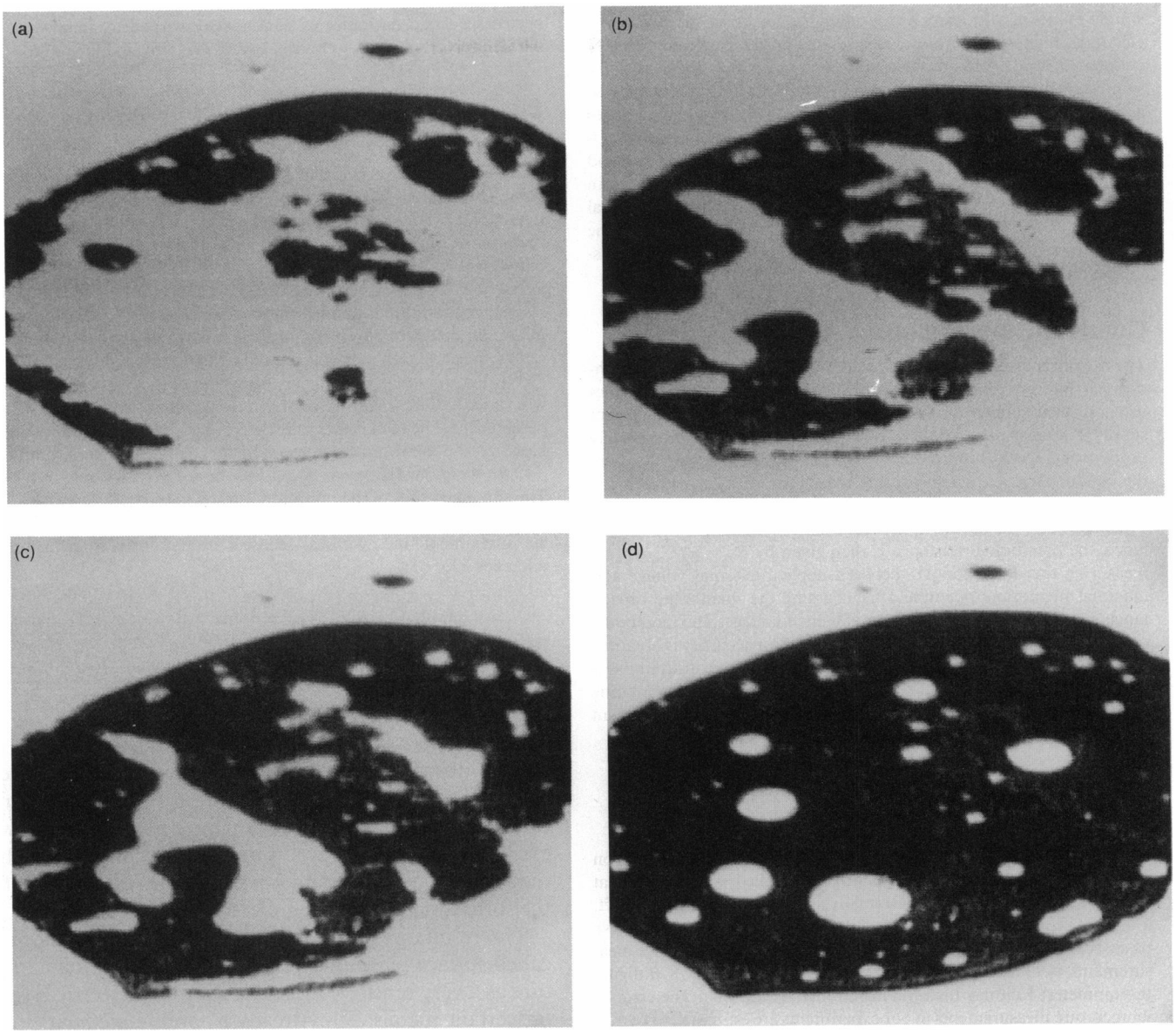

FIGURE 4 Thinning sequence of a PSM made from DOPC as seen in the SPM at (*a*) (*top left*) 30 s, (*b*) (*top right*) 60 s, (*c*) (*bottom left*) 120 s, (*d*) (*bottom right*) 30 min after applying potential pulses of ±100 mV. Parallel to the thinning of the membrane an increase of the capacitance was measured. The dark area corresponds to a monolayer of 24 Å. The white areas have a much higher thickness and are attributed to solvent lenses. Image size: 0.5 mm.

mV was applied between the gold film and a gold electrode in the electrolyte solution.

The incidence angle of the illumination in the surface plasmon microscope was chosen such that the resonance of the surface plasmon is at its maximum when the gold surface is covered by a film of refractive index $n = 1.48$ and 25 Å thickness, which are typical values for the lipid. So it was expected that wherever the film thinned to a monomolecular coverage, it would appear dark in the surface plasmon microscope.

Fig. 4 shows the thinning sequence of a lipid solvent droplet in the diaphragm. The experiment starts from a situation where no contrast at the surface is detectable. Then dark areas appear and grow slowly with time. In the case, in which DOPC was used, the thinning occurred only when voltage pulses were applied. With other lipid, this process occurred spontaneously. As will be discussed later in greater detail, this process depends sensitively on the nature of the lipid. The thickness of the surface layer in these dark areas was measured to be 24 Å. This value is within the experimental error of the thickness one would expect from a monomolecular lipid film on a HDM monolayer. Interestingly, the sequence shows that the film starts to thin from the rim of the diaphragm. This might have to do with the polarity of the rim. The remaining bright islands in the middle of

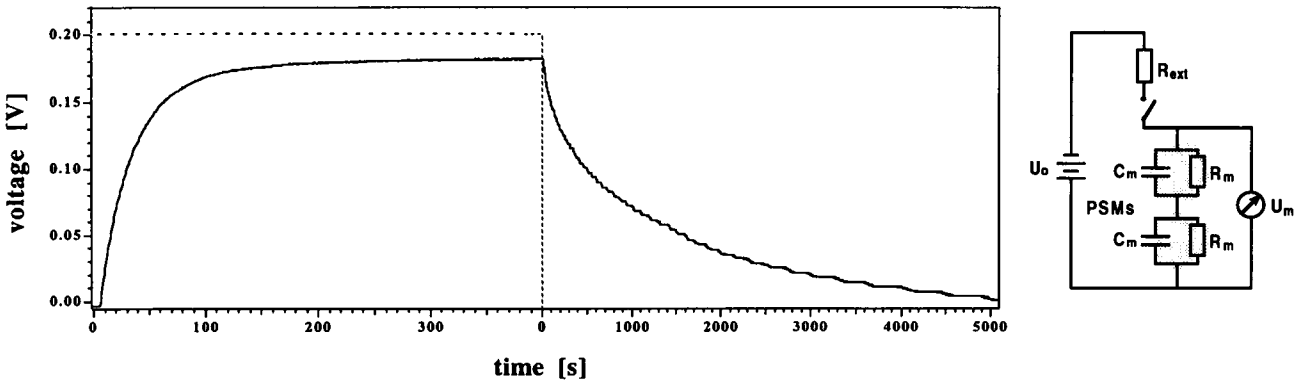

FIGURE 5 Potential change across a pair of PSMs during and after injection of charges. The diagram shows the schematics of the electrical circuit.

the field of view consist presumably of solvent. It is quite understandable that in this experimental geometry, where the film is oriented horizontally, the lenses are trapped and stable throughout the experiment. In cases where such a film is oriented vertically, as it is also the case with the BLM's, the gravity helps to drive the lenses out of the membrane (data not shown here).

Capacitance measurements, recorded in parallel to the thinning, showed the same time course as the optical experiment. Using an image analysis system, we measured the monomolecular areas and calculated the resulting specific capacitance from the measurements of the overall capacitance. The resulting value of 4.6 μF/cm^2 is again in good agreement with literature data obtained from symmetric BLM's (11).

In order to determine the electrical conductivity of the films, we started with a simplified symmetrical system. We used two of the above described PSM's which shared the same electrolyte solution but had separate gold electrodes. This symmetrical setup allowed us to measure conductivity and capacitance independently from the effects of the counter electrode. Fig. 5 shows the electrical circuit used for this approach. The membranes were charged via an external resistor, which was chosen to be on the order of the internal resistance of the membranes. The voltage across the membranes was measured with an electrometer, whose input resistance was higher than 10^{15} Ohm and thus negligible. As Fig. 5 shows, the voltage across the membranes increased slowly to a final value of 0.95 U_0. An exponential fit to the voltage increase (not shown) exhibited in most cases a very good agreement to a single exponential function with a characteristic relaxation time of $\tau = 35$ s. At higher voltages (above 500 mV) however, nonlinear effects were observed. At low voltages the charge-up time is determined only by the capacitance of the membrane and the external resistor. With an external resistor of $R = 1$ GΩ, the capacitance turned out to be $C = 3.5 \cdot 10^{-8}$ F/cm^2. This value which was determined in a quasi-static experiment fits well with the capacitance measured at higher frequencies. There is a tendency, however, that the capacitance measured at high frequencies appears to be slightly lower. With a known external resistor, the internal membrane resistance may be directly derived from the ratio of the end-value of the potential across the membranes: $R_i = (U/\Delta U - 1) \cdot R_e = 9 \cdot 10^9$ Ohm. This value converts with the known area to a specific conductivity of $1.6 \cdot 10^{-9}$ S/cm^2. When in the next step the external voltage source is disconnected, the charge difference across the membranes has to equilibrate via the internal resistance of the PSM. The decay constant is thus determined by the trans-membrane conductivity and the capacity. Again, the measured decay process turned out to be a single exponential function with a characteristic time constant of 1,300 s. With the known capacitance the trans-membrane specific conductivity is $3.8 \cdot 10^{-10}$ S/cm^2, which is even somewhat lower than the previously determined value. What counts here is the order of magnitude rather than the value itself. With these extremely low currents, already minor current leaks become significant error sources. It should also be noted here that the gold electrodes themselves have a significant resistivity towards the electrolyte solution. But this value is more than three orders of magnitude lower and may therefore be neglected in our considerations.

It is important to point out here, that this decay time has a very general meaning: it determines the practical applicability of such membranes. This relaxation time represents the time span over which charges may be stored across the membrane during an experiment, for example, by adsorbed electro-active entities like the ones used in the subsequent paper.

Conducting mechanism of the PSM

The above experiments show clearly that the lipid film has a drastic effect on the measured conductivity of the system. These measurements leave unclear, however, what the conduction mechanism through the membrane is. We have therefore employed cyclic voltammetry and measured the electrochemical turnover of certain redox species at our membrane coated electrodes. In the experimental setup the potential across the membrane was

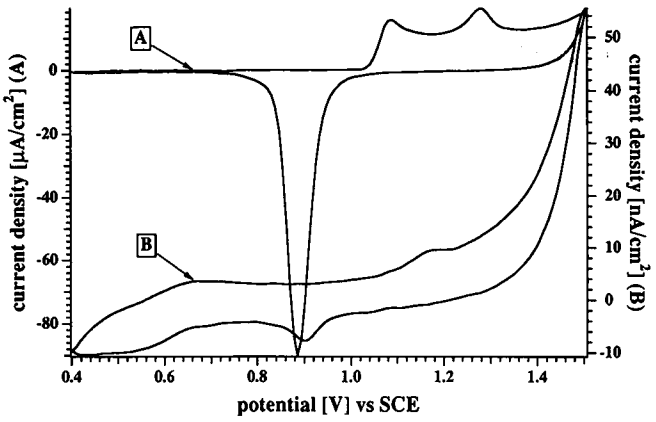

FIGURE 6 Cyclic voltammogram of a bare (*A*) and a HDM coated Au electrode (*B*) in 0.1 H_2SO_4 (scan rate 10 mV/s). The area under the oxide removal peak (~900 mV) is taken as an estimation of the coverage of the HDM coating.

now measured against a reference electrode and the current was driven through a working electrode. It should be noted however, that due to the low currents and the constancy in ionic strength and pH during the experiments, the use of a reference electrode instead of just a gold electrode is not mandatory. All control experiments (not shown here) have indicated that without the reference electrode, only the absolute potentials between the electrodes are shifted according to their different redox potentials.

Fig. 6 (trace *A*) shows the cyclic voltammogram of a bare gold electrode in 0.1 N sulfuric acid. The shape of the curve with its well pronounced oxide removal peak is typical for polycrystalline electrodes (12). The curve obtained under the same conditions from a gold film covered with HDM (trace *B*) is clearly different. It shows a pronounced hysteresis (which is due to the high capacitance) and most important shows a drastically reduced oxide removal peak. In many cases, the weak peak was not detectable any more. If one discusses the conduction mechanism across this organic film in terms of pinholes, then one can roughly estimate the fractional pinhole area in the HDM film from the areas under the oxide removal peaks (13, 14). With a peak-area ratio of $1.2 \cdot 10^{-9}$ AV/$6.1 \cdot 10^{-6}$ AV, the fraction of the surface of the pinholes would in this model be 0.0002. Because of the high offset current, this value should be seen as an upper limit.

In order to increase the sensitivity of our measurements we switched to a system with a high transfer rate. As can be seen in Fig. 7 *a*, the presence of the HDM layer does not completely suppress the redox cycle of the K_4FeCN_6. The current for this ion under the given conditions is only limited by the diffusion to the electrode and not by the electron transfer itself (15). As was found by Sabatini (14), the peak current for this ion reduces by less than 30% when the active surface area is reduced to as little as 0.0055. In our measurements we found a reduction of the current by more than two orders of magnitude by the HDM film (see Fig. 7 *a*, trace *A* and *B*). This means that in our measurements the free area must be extremely small. For a detailed discussion of the conduction mechanism in HDM film see also reference 16.

When covered with an additional lipid film, however, the redox currents are effectively suppressed. The formation of a PSM was confirmed by capacitance measurements. The remaining currents are rather insensitive to the presence of the redox species itself, as is shown in Fig. 7 *b*. This again indicates that the conduction through pinholes is negligable and other mechanism must be considered. From the slope of these cyclic voltammograms in the flat region between −300 mV and +300 mV, the conductivity of the PSM can again be calculated. It turns out to be $1.8 \cdot 10^{-9}$ S/cm².

In summary: the cyclic voltammetry measurements confirmed that these membranes are excellent electrical insulators. However, due to the extremely low currents, which are measured against the large capacitance of the membrane, it is extremely difficult to identify the charge

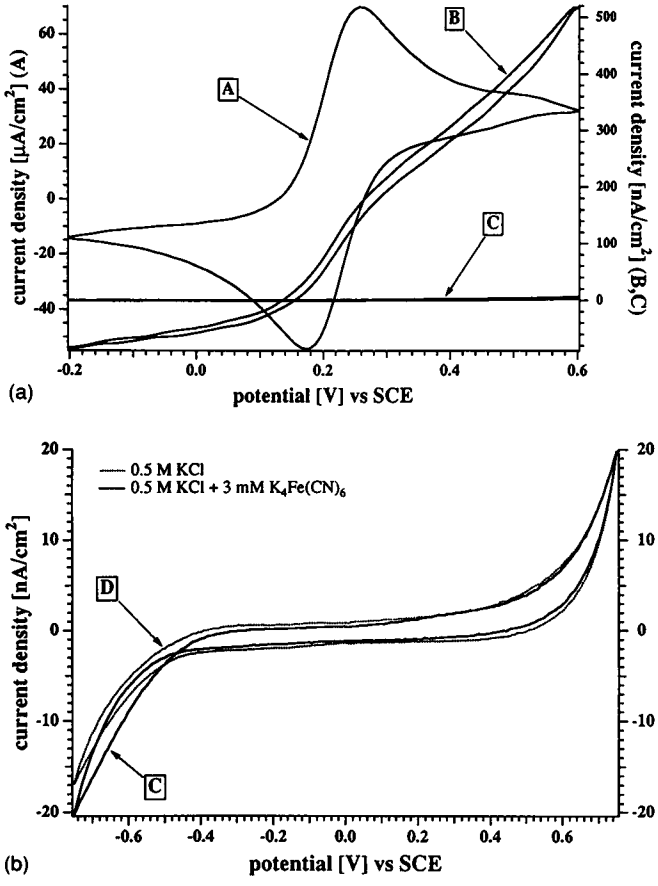

FIGURE 7 (*a*) Cyclic voltammogram of a bare Au electrode (*A*) the same electrode coated with HDM (*B*) and with a PSM made from DOPC (*C*) in 3 mM $K_4Fe(CN)_6$ and 0.5 M KCl. (*b*) magnified view of trace *C* and trace *D* recorded without $K_4Fe(CN)_6$. (Scan rate 10 mV/s.)

TABLE 1 **Specific capacitance, optical and electrical thickness, and specific conductivities of PSM's made from different lipids**

Lipid	C_{sp} [10^{-7} F/cm^2]	d_{el} [Å]	d_{opt} [Å]	λ_{sp} [nS/cm^2]
HDM	10.0	18.6*,‡	18.6	—
DLPC	6.9	27*	35.6§	9*
DMPC	5.9	32‡	39.6–41.6§	600*
DMPC*	—	—	—	8*
DOPC	4.6	40‡	42.6‖	7‡
DOPC	2.6–5.0	37–72*	—	30*
DPPC	5.7	36*	40.6‖	400*
DPPC	—	—	—	140‡

*,‡ Measurement methods given in the materials and methods section. §Measured with surface the plasmon spectrometer. ‖Measured with surface plasmon microscope. ¶Contains 5% fluorescent labelled DPPC.

transport mechanism or the transported species. This difficulty is also due to the fact that at these low currents impurities, which are hardly controllable, can dominate the redox processes. However, the experiments with K_4FeCN_6 clearly indicate that conduction through pinholes as mechanism is very unlikely. This in turn means that conduction through the membrane rather than through pinholes determines the charge transport.

Lipid-specific properties of the PSM

As we have seen in the previous sections, the properties of the PSM are largely determined by the lipid moiety of the film. It is therefore conceivable that specific properties of a particular lipid might be reflected in the properties of the membranes (17), or that characteristic physical properties of lipid films, which depend on external parameters like temperature or pH, might influence the properties of the PSM as a whole. As it turns out, it is a unique feature of the PSM compared with free standing films that a PSM may be composed of virtually every lipid, regardless of its liquid crystalline state.

In a first attempt we have compared PSMs made from lipids with different chains. Table 1 lists the various specific capacitances measured with low impedance based on the assumption of a simple RC circuit. A bare gold electrode shows a Helmholtz capacitance of about 40 μF/cm^2 (data not shown). The bare HDM layer exhibits a specific capacitance of 1μF/cm^2. Assuming a simple capacitor as a model, this capacitance corresponds to a thickness of 18.6 Å. Here the dielectric constant was taken to be $\epsilon = 2.1$. This value compares nicely with the expected thickness of the film with the chains tilted by 30° (6). With the various lipid films on top the capacitances are reduced significantly as listed in Table 1. The corresponding electrical thicknesses show a significant increase, which is correlated with the chain length. These values may be compared with the values determined by surface plasmon microscopy and spectroscopy. The data clearly show that the electrical thickness appears always to be smaller than the optical thickness of the PSM. This might be due to the penetration of ions into the head region of the lipid moiety with the result that the electric field "sees" not the whole length of the lipid molecule but rather only the hydrocarbon chain region. With this assumption the measured values would agree decently with the expected values. The accuracy of the thicknesses determined optically obviously depends sensitively on the homogeneity of the film. As the surface plasmons integrate over a distance of ~10 micrometer, microlenses smaller than this will contribute to the average thickness of the film. This might explain the much too large thickness measured by surface plasmon spectroscopy on DOPC films, which are known to retain a large amount of solvent in lenses (see Fig. 4). A quantitative analysis of the SPM images, where only the dark areas of films were taken into account, resulted in a more realistic value of the thickness (see Table 1).

Also listed in Table 1 are the specific conductivities of the various films. When listed with increasing chain length no pattern of conductivities is obvious. When listed with increasing chain melting temperature however, it becomes apparent that the films made from lipids, which in fully hydrated conditions are fluid at room temperature, show the lowest conductivity. This may easily be understood taking into account the high defect density in crystalline Langmuir-Blodgett films. On the other hand, the conductivities of PSMs made form lipids which in the crystalline state are still by one to two orders lower than the values which are reported from crystalline Langmuir-Blodgett films (18). This might be due to the fact that there is still enough organic solvent in the membranes which is partly trapped in the defects sealing them up. It should also be noted here that the different lipids exhibit quite drastic differences in the process of film formation from the organic solvent. The tendencies here are that films from lipids, which in fully hydrated conditions are in the crystalline state, form within seconds and contain less solvent. Films from lipids, which are fluid at room temperature, take up to several minutes to form and as judged by surface plasmon microscopy, contain solvent lenses.

In order to further assess the effects of the liquid crystalline state on the properties of the PSM, we investigated PSMs from DPPC as a function of the temperature. In Fig. 8 the specific capacitance and in Fig. 9 the specific conductance of DPPC is plotted as a function of temperature. Plotted in these figures is also the effect of the temperature change on the HDM layer itself. As Fig. 8 shows, temperature does not effect the capacitance of the HDM layer. It stays constant within the experimental error. The conductivity however increases exponentially with temperature indicating a thermally excited process. The capacitance as well as the conductivity of the PSM, show a strong temperature dependence and in contrast to the HDM layer, a pronounced and reproducible hysteresis. The massive change in the capacitance occurs between 35 and 45°C. This is several degrees lower than the main transition temperature (17) of the

pure and fully hydrated DPPC in vesicles. In our PSMs we have a hydrophobic coupling to the lower HDM layer, and we have a non negligible amount of trapped solvent in the film. The latter effect will tend to lower and broaden the phase transition and it may also contribute to the very pronounced hysteresis, as during crystallization of the lipid a large portion of the solvent will be squeezed out in a two-dimensional phase segregation. Future measurements of the lateral mobility in these PSM's will help to clarify these questions. Preliminary FRAP experiments with PSM's made from DMPC at 25°C (data not shown here) gave a diffusion coefficient between 5 and $8 \cdot 10^{-8}$ cm^2/s. This value is again in good agreement with mobilities measured in fully hydrated membranes (19).

CONCLUDING REMARKS

Despite their molecular thickness, painted supported membranes have shown to be extremely good electrical insulators. Due to their high mechanical stability PSM's open a broad variety of new experiments in the field of biophysics, physiology and electrochemistry. In contrast to conventional black lipid films which may be composed only by a very narrow range of lipids, the PSMs may consist of a broad variety of lipids. Moreover, it should be possible to reconstitute a broad variety of lipid anchored membrane proteins into these films allowing the study of certain functional aspects of these assemblies. Electro-active proteins in adsorbed membrane patches have already successfully been investigated and have shown to be fully functional on PSM's. Additional advantages of their design is that large areas of PSM's may be formed and that PSM's are accessible to surface sensitive techniques allowing selective studies of processes at the membrane. This should open new possibilities not only for their investigation but also for their local manipulation.

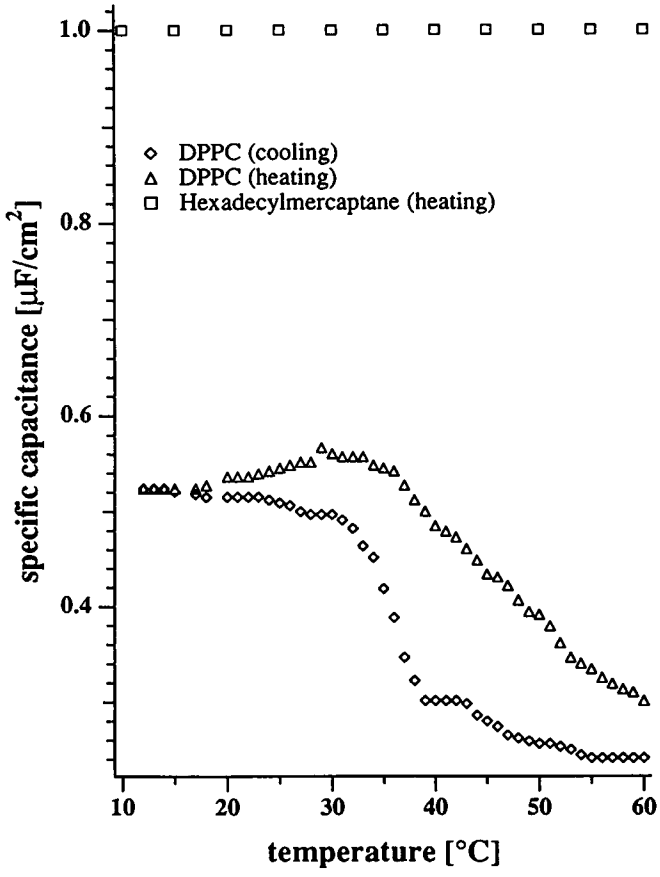

FIGURE 8 Specific capacitance as a function of the temperature of a HDM coated gold electrode and a PSM made from DPPC.

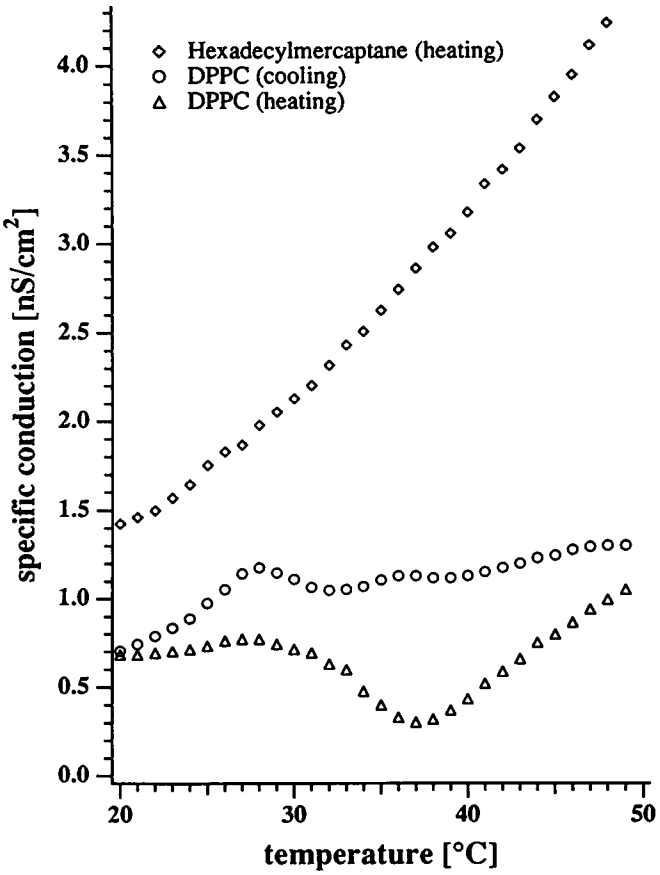

FIGURE 9 Specific conductivity as a function of the temperature for HDM coated gold electrode and a PSM made from DPPC.

This study was triggered by a very fruitful discussion with E. Bamberg, K. Fendler, and K. Seifert. We are in debt to Jerry Tsai for carefully reading this manuscript.

Received for publication 17 February and in final form 10 September 1992.

REFERENCES

1. Fromherz, P., and J. Klingler. 1989. An artificial membrane-cable: decay and delay of electrical potentials along a lipid bilayer with ion channels. *Biochim. Biophys. Acta.* 987:222–230.

2. Läuger, P., R. Benz, G. Stark, E. Bamberg, P. C. Jordan, A. Fahr, and W. Brock. 1981. Relaxation studies of ion transport systems in lipid bilayer membranes. *Quart. Rev. Biophys.* 14:513–598.
3. Läuger, P. 1987. Dynamics of ion transport systems in membranes. *Phys. Rev.* 67:1296–1331.
4. Mueller, P., D. O. Rudin, H. T. Tien, and W. C. Wescott. 1962. *Nature (Lond.).* 194:979–980.
5. Fromherz, P., C. Röcker, and D. Rüppel. 1986. From discoid micelles to spherical vesicles. The concept of edge activity. *Faraday Discuss. Chem. Soc.* 81:39–48.
6. Bain, C. D., E. B. Troughton, Y.-T. Tao, J. Evall, G. M. Whitesides, and R. G. Nuzzo. 1989. Formation of monolayer films by spontaneous assembly of organic thiols from solution onto gold. *J. Am. Chem. Soc.* 111:321–335.
7. Rothenhäusler, B., and W. Knoll. 1988. Surface-plasmon microscopy. *Nature (Lond.).* 332:615–617.
8. Fischer, B. 1988. Oberflächenplasmonen-mikroskopie und-spektroskopie an rekonstituierten Lipid/Protein-Membranen. diploma thesis. Technische Universität München.
9. Raether, H. 1977. Surface plasma oscillations and their applications, in Physics of thin films. G. Haas, M. H. Francombe, and R. W. Hoffmann, editors. Academic Press. 145–261.
10. Czaja, C., G. Jekutsch, B. Rothenhäusler, and H. E. Gaub. 1987. Formation of supported lipid/protein bilayers by surface induced vesicle fusion. *In* Biosensors. VCH Publishers, New York. 339–340.
11. Benz, R., O. Fröhlich, P. Läuger, and M. Montal. 1975. Electrical capacity of black lipid films and of lipid bilayers made from monolayers. *Biochim. Biophys. Acta.* 394:323–334.
12. Angerstein-Kozlowska, H., B. E. Conway, A. Hamelin, and L. Stoicoviciu. 1986. Elementary steps of electrochemical oxidation of single-crystal planes of au-I. Chemical basis of processes involving geometry of anions and the electrode surface. *Electrochim. Acta,* 31:1051–1061.
13. Sabatini, E., I. Rubinstein, R. Maoz, and J. Sagiv. 1987. Organized self-assembling monolayers on electrodes. Part I: octadecyl derivatives on gold. *J. Electroanal. Chem.* 219:365–371.
14. Sabatini, E., and I. Rubinstein. 1987. Organized self-assembling monolayers on electrodes. 2. Monolayer-based ultramicroelectrodes for the study of very rapid electrode kinetics. *J. Phys. Chem.,* 91:6663–6669.
15. Amatore, C., J. M. Saveánt, and D. Tessier. 1983. Charge transfer at partially blocked surfaces. A model for the case of microscopic active and inactive sites. *J. Electroanal. Chem.* 147:39–51.
16. Porter, M. D., T. B. Bright, D. L. Allara, and C. E. D. Chidsey. 1987. Spontaneously organized molecular assemlies. 4. Structural characterization of n-alkyl thiol monolayers on gold by optical ellipsometry, infrared spectroscopy, and electrochemistry. *J. Am. Chem. Soc.* 109:3559–3568.
17. Cevc, G., and D. Marsh. 1987. Phospholipid Bilayers. John Wiley and Sons, New York.
18. Stelzle, M., and E. Sackman. 1989. Sensitive detection of protein adsorption to supported lipid bilayers by frequency-dependent capacitance measurements and microelectrophoresis. *Biochim. Biophys. Acta.* 981:135–142.
19. Gaub, H. E., E. Sackmann, R. Büschl, and H. Ringsdorf. 1984. Lateral diffusion and phase separation in two-dimensional solutions of polymerized butadiene lipid in dimyristoysphosphatidylcholine bilayers. A photobleaching and freeze fracture study. *Biophys. J.* 45:725–731.